Piecewise linear emulator of the nonlinear Schrödinger equation and the resulting analytic solutions for Bose-Einstein condensates

Stavros Theodorakis*
Physics Department, University of Cyprus, P.O. Box 20537, Nicosia 1678, Cyprus

(Received 29 January 2003; published 9 June 2003)

We emulate the cubic term Ψ^3 in the nonlinear Schrödinger equation by a piecewise linear term, thus reducing the problem to a set of uncoupled linear inhomogeneous differential equations. The resulting analytic expressions constitute an excellent approximation to the exact solutions, as is explicitly shown in the case of the kink, the vortex, and a δ function trap. Such a piecewise linear emulation can be used for any differential equation where the only nonlinearity is a Ψ^3 one. In particular, it can be used for the nonlinear Schrödinger equation in the presence of harmonic traps, giving analytic Bose-Einstein condensate solutions that reproduce very accurately the numerically calculated ones in one, two, and three dimensions.

DOI: 10.1103/PhysRevE.67.066701 PACS number(s): 02.60.−x, 03.75.Hh, 03.65.Ge, 03.75.Lm

I. THE PIECEWISE LINEAR EMULATION

The discovery of Bose-Einstein condensates in vapors of alkali-metal atoms has prompted an increased interest in the cubic nonlinear Schrödinger equation. Indeed, the Gross-Pitaevskii equation, a highly successful three-dimensional mean field approximation that yields the macroscopic wave function for the gaseous Bose-Einstein condensates, is just a cubic nonlinear Schrödinger equation in a trapping potential. Nonlinear Schrödinger equations model many natural phenomena, ranging from light pulses in optical fibers to Bose-condensed photons. It is the trapping potential term, though, that has led to recent theoretical and mathematical investigations. Most of these investigations have focused on harmonic traps, which do not give analytic solutions, and have therefore consisted of numerical studies. Analytic solutions have been obtained for a finite square well [1], a double square well [2], an infinite square well [3], and a δ function potential [4]. The other potentials have been examined through variational and numerical methods. It would be desirable, therefore, to be able to obtain analytic solutions for these other potentials, even approximate ones. Such solutions would involve special functions in many cases, an unavoidable complication arising even when solving the linear Schrödinger equation. Nonetheless, they would provide an invaluable tool for studying the corresponding nonlinear phenomena.

In this paper we present a most general method for finding very good analytic approximate solutions to the cubic nonlinear Schrödinger equation. This method applies whenever the nonlinearity in that equation is a purely cubic one. It is most easily used when finding condensate ground states. It can be easily generalized though to higher states. It is also quite straightforward to generalize it so that it can handle nonlinear terms of any form.

The basic idea is to emulate the nonlinear Ψ^3 term by a piecewise linear function of Ψ, thus replacing the nonlinear Schrödinger equation by a set of linear inhomogeneous differential equations. These can be solved exactly, provided we are able to find a partial solution. This is possible in quite a few instances, as shown in the various examples presented below.

We should note that the idea of solving nonlinear boundary value problems by approximating terms of the differential equation and then patching local solutions at the knots has been used for finding numerical solutions to a number of boundary value problems [5]. Here, though, we focus on obtaining good analytic approximate solutions, rather than numerical ones.

Our piecewise linear emulation of the nonlinear Schrödinger equation involves then the replacement of the physically relevant piece of the cubic Ψ^3 curve with a corresponding circumscribed polygonal line, as shown in Fig. 1. Clearly, if this polygon consists of very many line segments, all of them tangent to the cubic curve, then the solution that will be obtained will be essentially the exact solution of the nonlinear problem. In practice, though, we shall replace the cubic curve by three line segments tangent to the curve. The resulting trilinear bicuspid curve is in fact a quite decent emulation of the Ψ^3 curve, as seen in Fig. 1.

Indeed, let us suppose that we are trying to find the ground state for a particular nonlinear Schrödinger equation in a certain trapping potential. Then we expect the wave function to tend to zero at infinity and to reach a maximum value Ψ_0 at a point that can be defined to be the origin $x=0$. We shall now approximate the curve Ψ^3 with an emu-

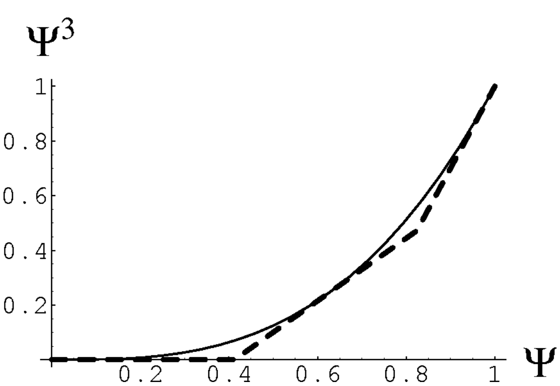

FIG. 1. The function Ψ^3 and its piecewise linear emulator f_{em}. The line segments are tangent to the curve at the points $\Psi=0$, $\Psi=s\Psi_0$, and $\Psi=\Psi_0$, where $s=(\sqrt{5}-1)/2$.

*Electronic address: stavrost@ucy.ac.cy

lator curve consisting of three straight line segments. These line segments will be tangent to the Ψ^3 curve at the points $\Psi=0$, $\Psi=s\Psi_0$, and $\Psi=\Psi_0$. In other words, we shall be replacing the cubic term with the emulator function f_{em}, where

$$f_{em}=\begin{cases} 0 & \text{if } 0\leqslant\Psi\leqslant\Psi_1, \\ 3s^2\Psi_0^2\Psi-2s^3\Psi_0^3 & \text{if } \Psi_1\leqslant\Psi\leqslant\Psi_2, \\ 3\Psi_0^2\Psi-2\Psi_0^3 & \text{if } \Psi_2\leqslant\Psi\leqslant\Psi_0. \end{cases} \tag{1}$$

Here s is a number between 0 and 1, while the two cusps of the emulator function occur at $\Psi_1=2s\Psi_0/3$ and $\Psi_2=2\Psi_0(1-s^3)/(3-3s^2)$.

The parameter s is chosen so as to make the emulator as similar as possible to the original. We thus select the value of s that minimizes the area between the cubic curve and the emulator polygonal line. This particular value turns out to be $s=(\sqrt{5}-1)/2$, in which case we get $\Psi_1=2s\Psi_0/3$ and $\Psi_2=4s\Psi_0/3$. Our emulator function is then fully specified and is indeed a very good simulacrum of the cubic curve, as seen in Fig. 1. It is this emulator function f_{em} of Eq. (1) that will be used in all of the following examples.

II. A ONE-DIMENSIONAL δ FUNCTION TRAP

We shall demonstrate the validity of our piecewise linear emulation by looking at various examples. We start by solving the nonlinear Schrödinger equation for the case of a δ function trap:

$$-\frac{\hbar^2}{2m}\frac{d^2\Psi}{dx^2}-\lambda\,\delta(x)\Psi+g|\Psi|^2\Psi=E\Psi, \tag{2}$$

where λ and g are positive. We measure Ψ in units of $(\lambda/\hbar)\sqrt{2m/g}$ and x in units of $\hbar^2/(2m\lambda)$, defining also the positive parameter $\beta=-\hbar^2E(2m\lambda^2)^{-1}$. The resulting dimensionless equation is

$$\frac{d^2\Psi}{dx^2}+\delta(x)\Psi-\Psi^3-\beta\Psi=0. \tag{3}$$

Here β is an externally given parameter. It can be fully determined if we require the particle number, which is proportional to the integral of the square of Ψ, to have a particular assigned value.

It is quite straightforward to find the ground state for this dimensionless equation. The exact ground state is found to be

$$\Psi=\sqrt{2\beta}\,\mathrm{cosech}\left(|x|\sqrt{\beta}+\sinh^{-1}\sqrt{\frac{4\beta}{1-4\beta}}\right), \tag{4}$$

whereby the maximum value Ψ_0 of the wave function Ψ is

$$\Psi_0=\sqrt{(1-4\beta)/2}=0.707\sqrt{1-4\beta}. \tag{5}$$

Let us now see if our emulator can reproduce this ground state solution. Thus we shall replace the cubic term in Eq. (3) with the emulator term f_{em} of Eq. (1). We shall be solving the ordinary differential equation

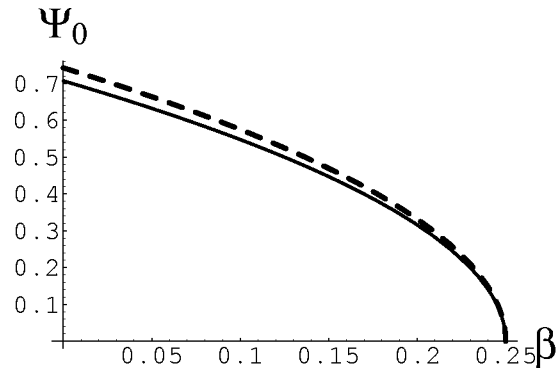

FIG. 2. The maximum value Ψ_0 of the wave function as a function of β in a δ trapping potential. The continuous curve corresponds to the exact solution, while the dashed curve corresponds to the piecewise linear emulation.

$$\frac{d^2\Psi}{dx^2}+\delta(x)\Psi-f_{em}-\beta\Psi=0, \tag{6}$$

the components of which are simply linear inhomogeneous ordinary differential equations. Each component must be solved in the corresponding interval, of course. Let us define the positive values x_1 and x_2, which are such that $\Psi(x_1)=\Psi_1=2s\Psi_0/3$, $\Psi(x_2)=\Psi_2=4s\Psi_0/3$, and $\Psi(0)=\Psi_0$. Then f_{em} is equal to zero when $|x|\geqslant x_1$, to $3s^2\Psi_0^2\Psi-2s^3\Psi_0^3$ when $x_2\leqslant|x|\leqslant x_1$, and to $3\Psi_0^2\Psi-2\Psi_0^3$ when $0\leqslant|x|\leqslant x_2$.

We solve Eq. (6) in each of the three intervals of the positive x axis, i.e., $[0,x_2]$, $[x_2,x_1]$, and $[x_1,\infty)$, making use of the fact that it suffices to find the ground state wave function just for non-negative values of x, since Ψ is even. Our solution involves nine unknown constants, namely, Ψ_0, x_1, x_2, and six constants of integration (two in each of the three regions). We shall impose the conditions that the wave function and its derivative be continuous at x_1 and x_2 (four conditions), that the wave function have the aforementioned appropriate values at the origin and at the points x_1 and x_2 (three conditions), that the derivative of the wave function have the appropriate discontinuity at the origin (one condition), and that the wave function vanish at infinity (one condition). There are thus nine equations and nine unknown constants. It is then quite straightforward to determine fully the solution of Eq. (6). We find from this piecewise linear emulation that the maximum value Ψ_0 of the wave function Ψ is

$$\Psi_0=\sqrt{(1-4\beta)}\sqrt{\frac{30\sqrt{5}+63}{236}}=0.742\sqrt{1-4\beta}. \tag{7}$$

This approximate result is very close to the exact result of Eq. (5), as can be seen in Fig. 2, where the maximum value of the wave function is plotted as a function of the parameter β.

The solution obtained from the piecewise linear emulation is

$$\Psi=\begin{cases}\Psi_1 e^{-\sqrt{\beta}(x-x_1)} & \text{if } x_1\leqslant x,\\ \dfrac{2s^3\Psi_0^3}{k^2}+\left(\Psi_2-\dfrac{2s^3\Psi_0^3}{k^2}\right)\cosh[k(x-x_2)]+(\Gamma d/k)\sinh[k(x-x_2)] & \text{if } x_2\leqslant x\leqslant x_1,\\ \dfrac{2\Psi_0^3}{d^2}+\gamma\cosh[d(x-x_2)]+\Gamma\sinh[d(x-x_2)] & \text{if } 0\leqslant x\leqslant x_2,\end{cases} \tag{8}$$

where $d^2=3\Psi_0^2+\beta$, $k^2=3s^2\Psi_0^2+\beta$, $\gamma=\Psi_2-(2\Psi_0^3/d^2)$, and $\Gamma=-2s\Psi_0\sqrt{k^2+3\beta}/(3d)$. The points x_1 and x_2 are given by the relations

$$\sinh[k(x_1-x_2)]=\frac{k}{k^2-\beta}\left(\frac{k^2+\beta}{\sqrt{\beta}}-\sqrt{3\beta+k^2}\right) \tag{9}$$

and

$$\sinh(dx_2)=\frac{1}{\gamma^2-\Gamma^2}[\gamma\Psi_0/(2d)+\Gamma(\Psi_0-(2\Psi_0^3/d^2))]. \tag{10}$$

Figure 3 shows the expression of Eq. (8), obtained from the piecewise linear emulation, as well as the exact ground state solution given by Eq. (4). We see that the two curves coincide. Thus the piecewise linear emulation does indeed succeed in providing us with a very accurate analytic approximation for the wave function of the ground state in the nonlinear Schrödinger equation with a δ function trapping potential.

III. THE KINK

Let us now demonstrate the validity of the piecewise linear emulation in a different context, namely, the domain wall between two equivalent phases. This domain wall is usually called a kink soliton.

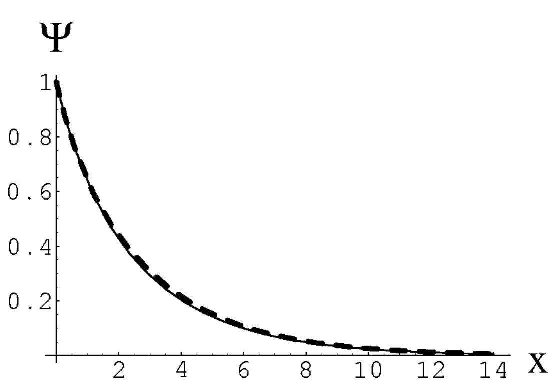

FIG. 3. The wave function for the ground state in a δ function trap, for $\beta=1/8$. The continuous line shows the exact result, while the dashed line shows the result given by the piecewise linear emulation.

We shall examine, in particular, the solution of the differential equation

$$\frac{d^2\Psi}{dx^2}-\Psi^3+\Psi=0, \tag{11}$$

subject to the boundary conditions $\Psi(\pm\infty)=\pm 1$. The kink that joins two equivalent homogeneous solutions of Eq. (11), the solutions 1 and -1, can be found exactly:

$$\Psi=\tanh(x/\sqrt{2}). \tag{12}$$

Let us see if we can reproduce this solution through a piecewise linear emulation. We may confine our attention to the positive x axis, since the kink will be an odd function. Thus the kink will have the value zero at $x=0$ and 1 at infinity. We emulate Eq. (11), then, by replacing the cubic Ψ^3 term with the term f_{em} of Eq. (1), the maximum Ψ_0 of the wave function being 1 in the present case. Thus the emulator Ψ is going to be the solution of

$$\frac{d^2\Psi}{dx^2}-f_{em}+\Psi=0, \tag{13}$$

where the emulator function f_{em} in this case is

$$f_{em}=\begin{cases}0 & \text{if } 0\leqslant x\leqslant x_1,\\ 3s^2\Psi-2s^3 & \text{if } x_1\leqslant x\leqslant x_2,\\ 3\Psi-2 & \text{if } x_2\leqslant x,\end{cases} \tag{14}$$

where the points x_1 and x_2 are defined by the expressions $\Psi(x_1)=2s/3$ and $\Psi(x_2)=4s/3$, s being always equal to $(\sqrt{5}-1)/2$. There are eight unknown constants, namely, x_1, x_2, and the six integration constants, two constants in each of the three regions that partition the positive x axis. These constants will be determined by the eight boundary conditions that have to be imposed. Indeed, we shall impose the conditions that the wave function and its derivative be continuous at x_1 and x_2 (four conditions), that the wave function take the values 0, $2s/3$, and $4s/3$, at the points 0, x_1, and x_2, respectively (three conditions), and that the wave function take the value 1 at infinity (one condition). There are thus eight equations and eight unknown constants. It is now a straightforward matter to solve exactly the resulting equations, obtaining

$$\Psi=\begin{cases} 1+\left(\frac{4s}{3}-1\right)e^{\sqrt{2}(x_2-x)} & \text{if } x_2\leqslant x, \\ \frac{2s^3}{3s^2-1}-1.5317e^{(x_2-x)p}-0.8803e^{(x-x_2)p} & \text{if } x_1\leqslant x\leqslant x_2, \\ \frac{2s}{3}\frac{\sin x}{\sin x_1} & \text{if } 0\leqslant x\leqslant x_1, \end{cases} \tag{15}$$

where $p=\sqrt{3s^2-1}$, and x_1 and x_2 turn out to be 0.5912 and 1.5574, respectively.

Figure 4 shows the expression for Eq. (15), obtained from the piecewise linear emulation, as well as the exact kink solution given by Eq. (12). We see that the two curves coincide. Thus the piecewise linear emulation does indeed succeed in providing us with a very accurate analytic approximation for the kink solution of Eq. (11).

IV. THE VORTEX

The previous two cases could be solved analytically, thus making the piecewise linear emulation superfluous. Most nonlinear Schrödinger problems cannot be solved analytically though, and it is in these cases that our method may prove to be invaluable.

An example of such a nonlinear problem that can be solved only numerically is the problem of a single vortex in a superfluid medium. The numerical solution of this problem is known [6]. The corresponding nonlinear Schrödinger equation is a two-dimensional differential equation:

$$-\frac{\hbar^2}{2m}\nabla^2\Psi+b|\Psi|^2\Psi-a\Psi=0. \tag{16}$$

For a vortex solution with a single quantum of circulation, Ψ takes the form $\psi(\rho)e^{i\phi}$, where ρ is the two-dimensional radius and ϕ is the azimuthal angle. If we measure the wave function in units of $\sqrt{a/b}$ and the radius in units of $\sqrt{\hbar^2/(2ma)}$, we obtain the ordinary differential equation

$$\frac{d^2\psi}{d\rho^2}+\frac{1}{\rho}\frac{d\psi}{d\rho}-\frac{1}{\rho^2}\psi-\psi^3+\psi=0. \tag{17}$$

We cannot obtain an exact analytic solution of this equation. It is in this case then that our method may prove to be quite useful.

We note first that ψ can take values between 0 at $\rho=0$ and 1 at infinity. So we shall replace the cubic term ψ^3 in Eq. (17) with the emulator term

$$f_{em}=\begin{cases} 0 & \text{if } 0\leqslant\rho\leqslant\rho_1, \\ 3s^2\psi-2s^3 & \text{if } \rho_1\leqslant\rho\leqslant\rho_2, \\ 3\psi-2 & \text{if } \rho_2\leqslant\rho, \end{cases} \tag{18}$$

where ρ_1 and ρ_2 are defined by the equations $\psi(\rho_1)=2s/3$ and $\psi(\rho_2)=4s/3$. It is then a straightforward matter to solve the resulting equations analytically, since we are dealing with linear inhomogeneous differential equations. There are eight unknown constants, namely, ρ_1, ρ_2, and six constants of integration, two in each of the three regions. The conditions that must be imposed arise from the continuity of the wave function and its derivative at ρ_1 and ρ_2 (four conditions), as well as from the fact that ψ takes the values 0, $2s/3$, $4s/3$, and 1 at 0, ρ_1, ρ_2, and infinity, respectively (four conditions). Thus all the unknown constants can be found, leading to an expression that involves Bessel functions and Struve L functions:

$$\psi=\begin{cases} \frac{\pi}{2}[I_1(\rho\sqrt{2})-L_1(\rho\sqrt{2})]-0.641\,326\;K_1(\rho\sqrt{2}) & \text{if } \rho_2\leqslant\rho, \\ -\pi s^3p^2L_1(\rho/p)+3.620\,77\,I_1(\rho/p)-0.002\,632\,45\;K_1(\rho/p) & \text{if } \rho_1\leqslant\rho\leqslant\rho_2, \\ 1.221\,15\;J_1(\rho) & \text{if } 0\leqslant\rho\leqslant\rho_1, \end{cases} \tag{19}$$

where $p=(3+\sqrt{5})/2$, $\rho_1=0.720\,578$, and $\rho_2=1.9686$. We can now use this approximation for the wave function of the vortex in order to calculate its energy. This energy is given by the expression

$$\int_0^R \pi\; d\rho(\rho\psi'^2+\psi^2/\rho+\rho\psi^4/2-\rho\psi^2). \tag{20}$$

If we use the approximation of Eq. (19) in order to calculate

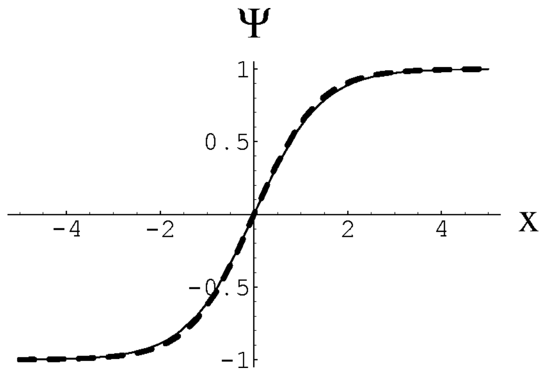

FIG. 4. The kink solution of Eq. (11). The continuous line shows the exact result of Eq. (12), while the dashed line shows the result given by the piecewise linear emulation.

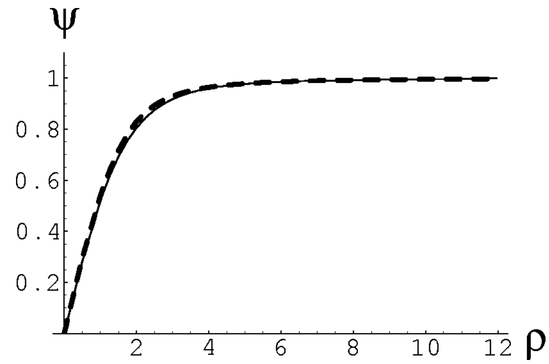

FIG. 5. The vortex solution of Eq. (17). The continuous line shows the exact numerical result, while the dashed line shows the result of Eq. (19) that was given by the piecewise linear emulation.

this energy, we shall find $\pi \ln(1.47R) - \pi R^2/4$. The energy obtained by solving the nonlinear Schrödinger equation (17) numerically [6] is identical to this, except for the number 1.47 being replaced by the number 1.46. The agreement between the two expressions is consequently excellent. This can also be seen in the plot of Fig. 5, where the wave function found by numerically solving the correct Eq. (17) coincides perfectly with the wave function of Eq. (19) that was obtained through the piecewise linear emulation. We conclude then that our emulation produces an excellent analytic simulacrum of the numerical solution.

V. THE *n*-DIMENSIONAL ISOTROPIC HARMONIC OSCILLATOR

In all the cases that were examined so far it was a relatively straightforward matter to solve exactly the linear inhomogeneous differential equations that resulted from the piecewise linear emulation. It will not always be easy to do that though, because there may be cases where a particular solution is hard to find. An additional difficulty will arise from the fact that the general solutions of the corresponding homogeneous differential equations may involve complicated special functions, in which case some symbolic computations may be necessary. In all cases, though, our emulation will provide us with a very good approximation for the functional form of the exact solution.

A good example of a nontrivial application of our method is the *n*-dimensional nonlinear Schrödinger equation in the presence of an isotropic harmonic trapping potential. This is the case relevant to the Bose-Einstein condensates. The wave functions for these condensates have been found only numerically [7–9]. We shall use the piecewise linear emulation in order to find analytic expressions for these solutions.

We shall be looking at the nonlinear Schrodinger equation

$$-\frac{\hbar^2}{2m}\nabla^2\Psi + \frac{1}{2}m\omega^2 r^2\Psi + g|\Psi|^2\Psi = E\Psi, \tag{21}$$

where g is positive (repulsive case). We shall concentrate on real ground state condensates and we shall measure Ψ in units of $\sqrt{\hbar\omega/(2g)}$, r in units of $\sqrt{\hbar/(m\omega)}$, and E in units of $\hbar\omega/2$. Then Eq. (21) reduces to the dimensionless equation

$$\frac{d^2\Psi}{dr^2} + \frac{n-1}{r}\frac{d\Psi}{dr} - r^2\Psi - \Psi^3 + E\Psi = 0, \tag{22}$$

where n is the dimension of the space and hence may take the values 1, 2, or 3.

We now proceed to the piecewise linear emulation of Eq. (22), replacing the cubic Ψ^3 term by the emulator f_{em} given by Eq. (1). We then have to solve the linear inhomogeneous equations

$$\frac{d^2\Psi}{dr^2} + \frac{n-1}{r}\frac{d\Psi}{dr} - r^2\Psi - f_{em} + E\Psi = 0. \tag{23}$$

We define the points r_1 and r_2, so that $\Psi(r_1) = 2s\Psi_0/3 = \Psi_1$, $\Psi(r_2) = 4s\Psi_0/3 = \Psi_2$, and $\Psi(0) = \Psi_0$, the parameter s having its standard value $s = (\sqrt{5}-1)/2$. Then Eq. (23) involves six unknown constants of integration (two in each one of the three regions) and three additional unknown parameters (Ψ_0, r_1, and r_2). These constants will be determined by the nine boundary conditions. Four conditions arise from the continuity of the wave function and its derivative at r_1 and r_2, two conditions arise at $r=0$ from the fact that the wave function acquires the maximum value Ψ_0 there, one condition arises from the fact that Ψ vanishes at infinity, and the last two conditions arise from the relations $\Psi(r_1) = 2s\Psi_0/3$ and $\Psi(r_2) = 4s\Psi_0/3$.

The solution of Eq. (23) in the region $r_1 \leqslant r$ is quite straightforward and is expressed in terms of the hypergeometric function U,

$$\Psi = \frac{2s\Psi_0}{3} e^{(r_1^2 - r^2)/2} \frac{U((n-E)/4, n/2, r^2)}{U((n-E)/4, n/2, r_1^2)}, \tag{24}$$

having made use of the boundary condition at infinity and of the known value $\Psi(r_1)$. The solutions in the other two regions are quite nontrivial, since a particular solution is not immediately obvious.

Let us begin with the inner region $(0 \leqslant r \leqslant r_2)$, where the wave function takes values between $4s\Psi_0/3$ and Ψ_0. The equation that has to be solved here is

$$\frac{d^2\Psi}{dr^2}+\frac{n-1}{r}\frac{d\Psi}{dr}-r^2\Psi-h^2\Psi+2\Psi_0^3=0, \tag{25}$$

with $h^2=3\Psi_0^2-E$. The solutions of the homogeneous equation are expressed in terms of hypergeometric functions: $e^{-r^2/2}{}_1F_1((n+h^2)/4,n/2,r^2)$ and $e^{-r^2/2}U((n+h^2)/4,n/2,r^2)$. However, the hypergeometric U piece diverges at $r=0$ when $n=2$ or 3, and gives a finite nonzero slope there when $n=1$, making it impossible for Ψ to have its maximum there. The U piece must be excluded therefore, since the ground state has to be even about the origin. We are left with the other hypergeometric piece, the piece containing the so called Kummer function. Thus we know the general solution.

We need, however, a particular solution of the full inhomogeneous equation in order to obtain the full analytic solution. Such a solution is not immediately obvious. We can find it, though, if we concentrate our attention on the nonlinear region, where we expect large Ψ_0 values. Indeed, let us define the variable $w=1/(r^2+h^2)$. For large values of Ψ_0 this is small everywhere and we shall be able to write down convergent series in terms of this variable. In fact, Eq. (25) can be rewritten in the form

$$(4w^4-4h^2w^5)\frac{d^2\Psi}{dw^2}+[(8-2n)w^3-8h^2w^4]\frac{d\Psi}{dw}-\Psi+2w\Psi_0^3=0. \tag{26}$$

The solution of this equation for small w is

$$\phi_{in}=2\Psi_0^3[w+(8-2n)w^3-8h^2w^4]+O(w^5). \tag{27}$$

This relation indicates that for small w, when we may keep only the term of order w, we have to have $\Psi_0^2\approx E$, since Ψ acquires the value Ψ_0 at the origin.

Equation (27) is a partial solution of Eq. (25), the full solution of which now takes the form

$$\Psi=\phi_{in}(r)+\left(\frac{4s\Psi_0}{3}-\phi_{in}(r_2)\right)\times e^{(r_2^2-r^2)/2}\frac{{}_1F_1((n+h^2)/4,n/2,r^2)}{{}_1F_1((n+h^2)/4,n/2,r_2^2)}. \tag{28}$$

We can use a similar approach for the region $r_2\leqslant r\leqslant r_1$ in the middle. The equation that must be solved here is

$$\frac{d^2\Psi}{dr^2}+\frac{n-1}{r}\frac{d\Psi}{dr}-r^2\Psi-j^2\Psi+2s^3\Psi_0^3=0, \tag{29}$$

where $j^2=3s^2\Psi_0^2-E$. For large Ψ_0 an approximate partial solution can be obtained in the same manner as the one used in the inner region. This partial solution is

$$\phi_{mid}=2s^3\Psi_0^3[y+(8-2n)y^3-8j^2y^4], \tag{30}$$

where $y=1/(r^2+j^2)$. The full solution in this region turns out to be

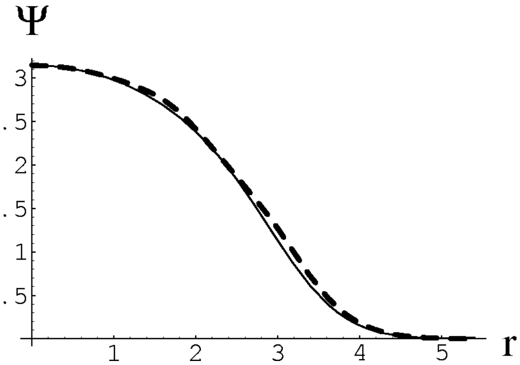

FIG. 6. The solution of Eq. (22) for $n=1$ and $E=10$. The continuous line shows the exact numerical result, while the dashed line shows the result that is given by the piecewise linear emulation.

$$\Psi=\phi_{mid}(r)+Ae^{-r^2/2}{}_1F_1((n+j^2)/4,n/2,r^2)+Be^{-r^2/2}U((n+j^2)/4,n/2,r^2). \tag{31}$$

The constants A and B can be found by requiring Ψ to take the appropriate values at the points r_1 and r_2. Hence $A=A_1/C$ and $B=B_1/C$, where

$$A_1=e^{r_2^2/2}[-\phi_{mid}(r_2)+(4s/3)\Psi_0]U((n+j^2)/4,n/2,r_1^2)-e^{r_1^2/2}[-\phi_{mid}(r_1)+(2s/3)\Psi_0]U((n+j^2)/4,n/2,r_2^2), \tag{32}$$

$$B_1=e^{r_1^2/2}[-\phi_{mid}(r_1)+(2s/3)\Psi_0]\,{}_1F_1((n+j^2)/4,n/2,r_2^2)-e^{r_2^2}[-\phi_{mid}(r_2)+(4s/3)\Psi_0])\,{}_1F_1((n+j^2)/4,n/2,r_1^2), \tag{33}$$

and

$$C={}_1F_1((n+j^2)/4,n/2,r_2^2)U((n+j^2)/4,n/2,r_1^2)-{}_1F_1((n+j^2)/4,n/2,r_1^2)U((n+j^2)/4,n/2,r_2^2). \tag{34}$$

Equations (24), (28), and (31) describe fully the solution given by the piecewise linear emulation. The remaining unknown quantities (r_1, r_2, and Ψ_0) will be determined by requiring that the derivative of the wave function be continuous at r_1 and r_2, and that $\Psi(0)=\Psi_0$. Of course, our solution will be a function of the input parameter E, which is determined by the total number of particles.

Figure 6 shows a comparison of the numerically obtained solution to the solution given by the piecewise linear emulation in one dimension ($n=1$), for $E=10$, a value of E that is large enough to ensure the validity of the partial solutions of Eq. (27) and Eq. (30). We see that our approximation reproduces very closely the numerically obtained exact result.

Figure 7 shows a comparison of the numerically obtained solution to the solution given by the piecewise linear emulation in two dimensions ($n=2$), for $E=10$. We see that the approximation reproduces very closely the numerically obtained exact result.

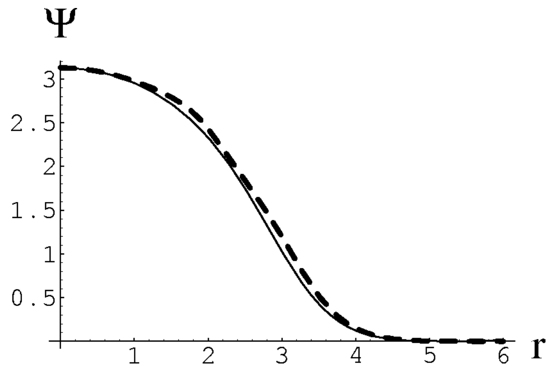

FIG. 7. The solution of Eq. (22) for $n=2$ and $E=10$. The continuous line shows the exact numerical result, while the dashed line shows the result that is given by the piecewise linear emulation.

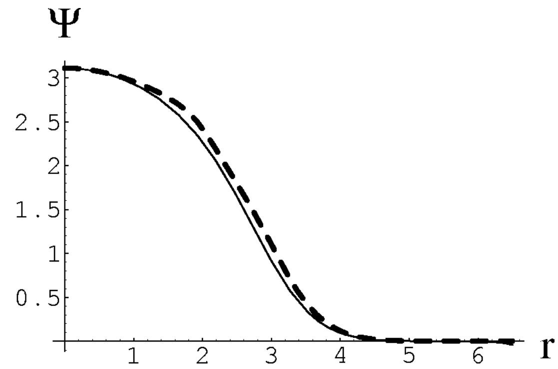

FIG. 8. The solution of Eq. (22) for $n=3$ and $E=10$. The continuous line shows the exact numerical result, while the dashed line shows the result from the piecewise linear emulation.

Finally, Fig. 8 shows a comparison of the exact numerical solution to the approximate analytic solution given by the piecewise linear emulation in three dimensions ($n=3$), for $E=10$. We see that the approximation again reproduces very closely the numerical result.

VI. CONCLUSIONS

In all the examples discussed we saw that a piecewise linear emulation of a nonlinear Schrödinger differential equation can give a very accurate analytic expression for the ground state, even when the emulator curve is just a bicuspid one. There are cases, of course, when the emulation will have to involve more pieces. These are the cases with higher states or with nonlinearities consisting of multiple and possibly more complicated terms. The basic criterion is always whether the graph of the piecewise linear approximation is a satisfactory simulacrum of the graph of the original nonlinear terms. This will always be the case if the emulator consists of enough linear segments. With the cubic term three segments are quite sufficient. More complicated nonlinear terms will need an emulator with more than two cusps and more than three pieces. Furthermore, while our approximate scheme should work quite well for static situations, it may not work in the case of nonequilibrium situations examined by time-dependent differential equations, since phase errors will accumulate with time and may matter quite a bit. Nevertheless, the piecewise linear emulation we presented can have a ubiquitous presence, since it can deal with very many nonlinear problems, especially static ones. The resulting analytic expressions can provide a very useful handle in dealing with such problems. The expression of Eq. (19) for the vortex is a good example of a very good approximation for a curve that is accessible only through variational or numerical work.

[1] L.D. Carr, K.W. Mahmud, and W.P. Reinhardt, Phys. Rev. A **64**, 033603 (2001).
[2] K.W. Mahmud, J.N. Kutz, and W.P. Reinhardt, Phys. Rev. A **66**, 063607 (2002).
[3] L.D. Carr, Charles W. Clark, and W.P. Reinhardt, Phys. Rev. A **62**, 063610 (2000).
[4] Stavros Theodorakis and Epameinondas Leontidis, J. Phys. A **30**, 4835 (1997).
[5] R.C.Y. Chin and R. Krasny, SIAM (Soc. Ind. Appl. Math.) J. Sci. Stat. Comput. **4**, 229 (1983).
[6] V.L. Ginzburg and L.P. Pitaevskii, Zh. Éksp. Teor. Fiz. **34**, 1240 (1958) [Sov. Phys. JETP **7**, 858 (1958)].
[7] Mark Edwards and K. Burnett, Phys. Rev. A **51**, 1382 (1995).
[8] M. Kunze, T. Kupper, V.K. Mezentsev, E.G. Shapiro, and S. Turitsyn, Physica D **128**, 273 (1999).
[9] Yuri S. Kivshar and Tristram J. Alexander, e-print cond-mat/9905048; Luc Berge, Tristram J. Alexander, and Yuri S. Kivshar, Phys. Rev. A **62**, 023607 (2000); Yuri S. Kivshar, Tristram J. Alexander, and Sergey K. Turitsyn, Phys. Lett. A **278**, 225 (2001).